Application of Zakharov equation in three dimensions to deep water gravity waves

Article *in* International journal of physical sciences · December 2011

DOI: 10.5897/IJPS11.682

CITATIONS
2

READS
40

4 authors, including:

Cesar Mbane Biouele
University of Yaounde I
33 PUBLICATIONS **104** CITATIONS

SEE PROFILE

International Journal of the Physical Sciences Vol. 6(33), pp. 7447 - 7455, 9 December, 2011
Available online at http://www.academicjournals.org/IJPS
DOI: 10.5897/IJPS11.682
ISSN 1992 - 1950 ©2011 Academic Journals

Full Length Research Paper

Application of Zakharov equation in three dimensions to deep water gravity waves

Stéphane ATOCK A. NWATCHOK, César MBANE BIOUELE*, Bernard ESSIMBI ZOBO and Théodule NKOA NKOMOM

Department of Physics, University of Yaoundé I, P.O. Box 812 Yaoundé-Cameroun.

Accepted 26 July, 2011

A numerical method, based on the Zakharov equation in three dimensions, is developed to study the nonlinear dynamics of deep water gravity waves. We focus primarily on systems describing the evolution of hydrodynamic surface waves, considering a thick incompressible fluid spanning across all space available and subject to gravity. The reference height to the resting state is z = 0. In the case of hydrostatic equilibrium, the bottom of the water is located at a distance H from the water surface. This depth is considered constant. The height of the surface wave is denoted η(x,y,t) and the volume occupied by the fluid is restricted by –H < z < η(x,y,t). This study shows that rogue waves are generated by primary waves whose directions of propagation are nearly parallel (i.e. 0 < θ < π/6). This ensures their unexpected character (expressed by the quasi-spontaneous passage from a calm situation to a sea greatly agitated).

Key words: Zakharov equation, nonlinear dynamics, deep water gravity waves.

INTRODUCTION

Since seamen roam the oceans, they are impressed by these huge rivers relatively hostile that inspires respect and fear. As evidence of this fear, many legends have always circulated such stories, expressing the existence of mermaids' shipwrecks (Touboul, 2007; Chambarel, 2009). The ghost ships savagely attack ships, or even beliefs about the Bermuda Triangle, where ships disappear inexplicably. Among these legends, is that of rogue waves that correspond in many respects to deep water gravity waves (Touboul, 2007). Many accounts of seamen have alluded to walls of water rising for no reason in the middle of the sea and hitting ships with extraordinary violence. These stories were not credible until 1978, when the cargo ship "Munchen" disappeared under mysterious circumstances. This vessel at the forefront of naval technology was heading in the North Atlantic, with no apparent problems until the night of December 12. Given that the weather service recorded no storm that night, it is reasonable to believe that a rogue wave is the only plausible explanation for this shipwreck. In 1980 (Chambarel, 2009), Philippe Lijour, captain of the tanker "Esso Lanuedoc" demonstrated the existence of rogue waves with a photo as proof. The existence of rogue waves is now universally recognized (Onorato et al., 2004; Socquet et al., 2005; Dyachenko and Zakharov, 2005; Kharif and Pelinovsky, 2003; Wu and Yao, 2004; White and Fornberg, 1998), and many images on the extent of damage caused by these monsters of the ocean are available online on the Internet. However, the physical processes responsible for the formation and spread of the phenomenon as well as its prediction are not completely understood. Contrary to popular belief Mbane (2009) demonstrated that, the natural phenol-menon like rogue waves are not just spectacular events accessible to routine observations and satellites images. Rogue waves are a combination of complex physical processes that occur under the accuracy conditions. Numerical computations (Atock et al., 2010; Shener, 2010; Leblanc, 2008; Batra et al., 2006; Trulsen et al., 2000) offers tremendous opportunities for understanding of the physical phenomena whose analytical solutions are, at the present stage of development of mathematics, difficult to obtain. Our paper presents the application of

*Corresponding author: E-mail: cesar.mbane@yahoo.fr. Tel: (+237) 77 40 49 23.

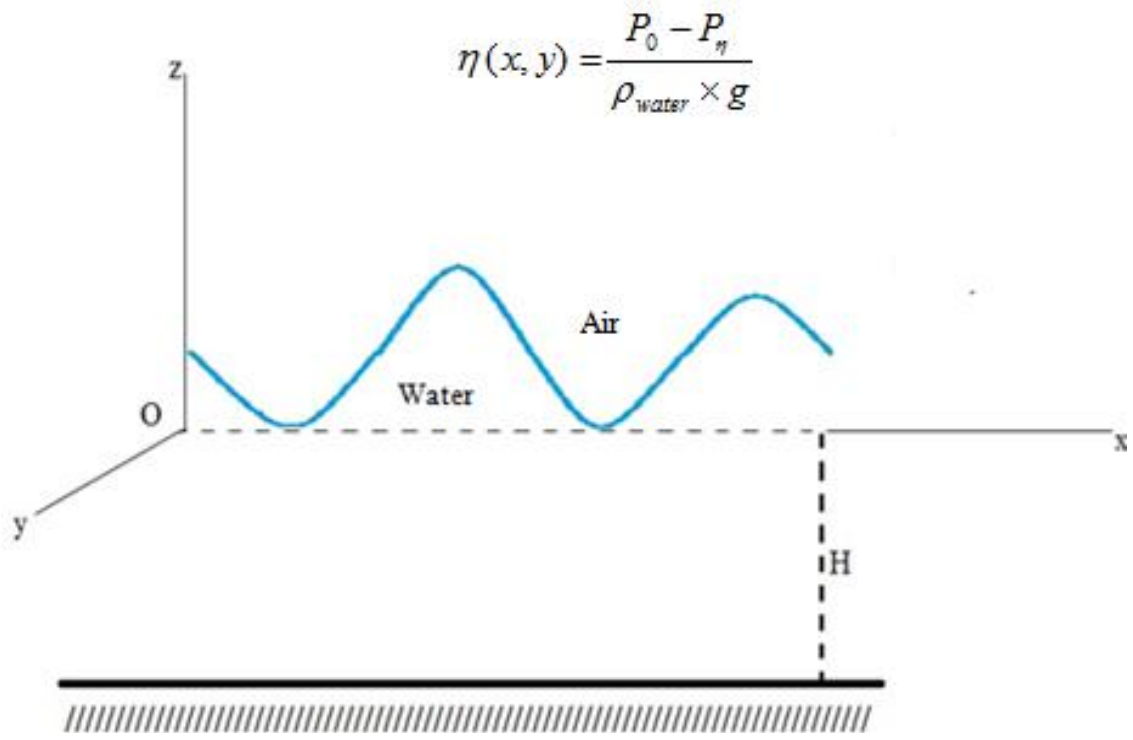

Figure 1 . Sketch of the study area. The height of the surface wave denoted η(x,y,t) is proportional to: (i) The difference between the atmospheric pressure at z = 0 and z = η; (ii)The temperature of ocean surface (that is, the density, ρ, of water decreases as temperature increases).

Zakharov equation in three dimensions to deep water gravity waves, which is an important tool for acquiring information on the scientifically conceivable reasons of formation of rogue waves. In this regard, additional assumptions are implemented to make the transition from hydrodynamic Euler equations to Sakharov's modulation instability. The study area is schematically shown in Figure 1.

BASIC FORMULATION OF ZAKHAROV EQUATION

Additional assumptions

The general fluid continuity equation is given by:

$$\frac{\partial\rho}{\partial t}+\frac{\partial\rho u}{\partial x}+\frac{\partial\rho v}{\partial y}+\frac{\partial\rho w}{\partial z}=0 \quad (1)$$

This leads to the continuity equation for an incompressible fluid

$$\frac{\partial u}{\partial x}+\frac{\partial v}{\partial y}+\frac{\partial w}{\partial z}=0 \quad (2)$$

The velocity perpendicular to the surface of the water and to the impermeable bottom is zero:

$$\vec{V}.\vec{n}=0 \text{ , at z = -H or z = } \eta \quad (3)$$

Here $\vec{n}$ is the unit vector normal to the surface. When the bottom is parallel to the undisturbed surface

$$w = 0, z = -H \quad (4)$$

And the kinematic boundary condition at the surface becomes

$$\left(u,v;w-\frac{\partial\eta}{\partial t}\right).\left(-\frac{\partial\eta}{\partial x},\frac{\partial\eta}{\partial y},1\right)=0,$$

$$z=\eta \Rightarrow w=\frac{\partial\eta}{\partial t}+u\frac{\partial\eta}{\partial x}+v\frac{\partial\eta}{\partial y} \quad (5)$$

where the surface of the water is allowed to change with time. The last condition comes from the Newtonian force on a moving fluid element

$$\frac{\partial\vec{V}}{\partial t}+(\vec{V}.\vec{\nabla})\vec{V}=\nu((\vec{\nabla}.\vec{\nabla})\vec{V})-\frac{1}{\rho}\vec{\nabla}P+\vec{g} \quad (6)$$

For an inviscid fluid this simplifies to

$$\frac{\partial \vec{V}}{\partial t} + (\vec{V}.\vec{\nabla})\vec{V} = -\frac{1}{\rho}\vec{\nabla}P + \vec{g} \quad (7)$$

When the flow is irrotational

$$\vec{\nabla}.\vec{V} = 0 \quad (8)$$

The velocity potential is also given by

$$\vec{V} = (u,v,w) = \left(\frac{\partial \phi}{\partial x}, \frac{\partial \phi}{\partial y}, \frac{\partial \phi}{\partial z}\right) = \vec{\nabla}\phi \quad (9)$$

Given the continuity equation

$$\frac{\partial^2 \phi}{\partial x^2} + \frac{\partial^2 \phi}{\partial y^2} + \frac{\partial^2 \phi}{\partial z^2} = \Delta\phi = 0 \quad (10)$$

The kinematic boundary condition at the bottom

$$\vec{\nabla}\phi.\vec{n} = 0 \text{ , z = -H} \quad (11)$$

The kinematic boundary condition at the surface

$$\frac{\partial \phi}{\partial z} = \frac{\partial \eta}{\partial t} + \nabla_\perp \phi.\nabla_\perp \eta \text{ , z = } \eta \quad (12)$$

Integrating equation (7) with respect to x,y,z, one can get the Bernoulli equation, the arbitrary functions of integration $C_1(y,z,t)$, $C_2(x,z,t)$, $C_3(x,y,t)$ must be the same function C(t), which can be absorbed by the velocity potential, yielding exactly the same flow

$$\frac{\partial \phi}{\partial t} + \frac{1}{2}\left(\vec{\nabla}\phi\right)^2 + g\eta = -\frac{P}{\rho} \text{ , z = } \eta \quad (13)$$

Here we have made the assumption that $\vec{g}$ is constant $\vec{g} = (0,0,-g)$ making the gravitational force conservative and making it possible to define a potential energy. Furthermore, we have made the assumption that the surface tension can be neglected. At the surface, z = η, for water flows the space above the water is the atmosphere where the density of air is only about 1/800 times that of water and the pressure is almost constant along the surface. Since this constant pressure has no important influence on the solution, we can put P=0, thus the dynamical boundary condition at the surface of the water becomes

$$\frac{\partial \phi}{\partial t} + \frac{1}{2}\left(\vec{\nabla}\phi\right)^2 + g\eta = 0 \text{ , z=}\eta \quad (14)$$

Equation 10, 11, 12 and 14 are basis for all the following calculations. By introducing the stream function $\psi(x,y,t)$, defined by $\psi(x,y,t) = \phi(x,y,\eta,t)$, Equations 12 and 14 become:

$$\eta_t + \left(\vec{\nabla}\ \eta\right).\left(\vec{\nabla}_\perp \psi\right) - \phi_z\left(1 + \left(\vec{\nabla}_\perp \eta\right)^2\right) = 0 \quad (15)$$

$$\psi_t + g\eta + \frac{1}{2}\left(\vec{\nabla}_\perp \psi\right)^2 - \frac{1}{2}\phi^2\left(1 + \left(\vec{\nabla}_\perp \eta\right)^2\right) = 0 \quad (16)$$

Materialization of the 3D interface between Euler and Zakharov equations

Zakharov equations were obtained for the first time in 1968 for ultra deep waters (Zakharov, 1968) and for deep waters by Zakharov and Kharitonov (1970). We will get those Zakharov equations starting from the considerations of Yuen and Lake (1980). The use of kinematic boundary conditions (Equation11 and 12) and dynamic (Equation 14), and the Fourier transform of the Dirac δ function and the development in Taylor series of hyperbolic functions yields the Fourier transform of the stream function $\psi(x,y,t)$ at the free surface of water:

$$\overline{\psi} = \overline{\phi} + \frac{1}{2\pi}\iint \overline{\phi}_1 \tanh(k_1 H)\vec{k}_1 \overline{\eta}_2 \delta\left(\vec{k}_1 + \vec{k}_2 - \vec{k}\right)d\vec{k}_1 d\vec{k}_2 + \quad (17)$$
$$\frac{1}{(2\pi)^2}\iiint \overline{\phi}_1 \frac{k_1^2}{2}\overline{\eta}_2 \overline{\eta}_3 \delta\left(\vec{k}_1 + \vec{k}_2 + \vec{k}_3 - \vec{k}\right)d\vec{k}_1 d\vec{k}_2 d\vec{k}_3 + \ldots$$

Equation 17 is inverted iteratively. It is natural to choose the starting guess as

$\overline{\phi}^{(1)} = \overline{\psi}$. Then,

$$\overline{\phi} = \overline{\psi} - \frac{1}{2}\iint k_1 \tanh\left(\vec{k}_1 H\right)\overline{\psi}_1 \overline{\eta}_2 \delta\left(\vec{k}_1 + \vec{k}_2 - \vec{k}\right)d\vec{k}_1 d\vec{k}_2 d\vec{k}_1 d\vec{k}_2 - \quad (18)$$
$$\frac{1}{(2\pi)^2}\iiint \frac{1}{4}k_1 \overline{\psi}_1 \overline{\eta}_2 \overline{\eta}_3 (2k_1 - \tanh(k_1 H)$$
$$\left(\left|\vec{k}_1 + \vec{k}_2\right|\tanh\left(\left|\vec{k}_1 + \vec{k}_2\right|H\right) + \left|\vec{k}_1 + \vec{k}_2\right|\tanh\left(\left|\vec{k}_1 + \vec{k}_2\right|H\right) + \right.$$
$$\left.\left|\vec{k} - \vec{k}_2\right|\tanh\left(\left|\vec{k} - \vec{k}_2\right|H\right) + \left|\vec{k} - \vec{k}_3\right|\tanh\left(\left|\vec{k} - \vec{k}_3\right|H\right)\right))$$
$$\delta\left(\vec{k}_1 + \vec{k}_2 + \vec{k}_3 - \vec{k}\right)d\vec{k}_1 d\vec{k}_2 d\vec{k}_3 - \ldots$$

The Fourier transform of the velocity vector at the water surface is given by (19):

$$\bar{v} = \overline{\psi} k \tanh(kH) - \frac{1}{2\pi}\iint \left(k \tanh(kH) k_1 \tanh(k_1 H) - k_1^2\right)\overline{\psi}_1 \overline{\eta}_2 \delta\left(\vec{k}_1 + \vec{k}_2 + \vec{k}_3 - \vec{k}\right) d\vec{k}_1 \quad (19)$$
$$\frac{1}{(2\pi)^2}\iiint \frac{1}{4}\overline{\psi}_1 \overline{\eta}_2 \overline{\eta}_3 k_1 (k \tanh(kH)(2k_1 - \tanh(k_1 H)$$
$$\left(\left|\vec{k}_1 + \vec{k}_2\right| \tanh\left(\left|\vec{k}_1 + \vec{k}_2\right| H\right) + \left|\vec{k}_1 + \vec{k}_3\right| H) \tanh\left(\left|\vec{k}_1 + \vec{k}_3\right| H\right) +$$
$$\left|\vec{k} - \vec{k}_2\right| \tanh\left(\left|\vec{k} - \vec{k}_2 H\right|\right) + \left|\vec{k} - \vec{k}_3\right| \tanh\left(\left|\vec{k} - \vec{k}_3\right| H\right)\ )) +$$
$$\tanh(k_1 H)\left(2k^2 - 4\vec{k}_2 . \vec{k}_3\right)\delta\left(\vec{k}_1 + \vec{k}_2 + \vec{k}_3 - \vec{k}\right) d\vec{k}_1 d\vec{k}_2 d\vec{k}_3 - \ldots$$

Equation 15 and 16 are modified using relations 17, 18 and 19, to obtain the Fourier transforms of the dynamic and kinematics boundary conditions.

$$\overline{\eta}_t - \overline{\psi}\frac{\omega^2}{g} + \frac{1}{2\pi}\iint\left(\frac{\omega^2}{g}\frac{\omega_1^2}{g} - \vec{k}.\vec{k}_1\right)\overline{\psi}_1 \overline{\eta}_2 \delta\left(\vec{k}_1 + \vec{k}_2 - \vec{k}\right) d\vec{k}_1 d\vec{k}_2 \quad (20)$$
$$\frac{1}{16\pi^2}\iiint\left(2k^2\frac{\omega_1^2}{g} + 2k_1^2\frac{\omega^2}{g} - \frac{\omega^2}{g}\frac{\omega_1^2}{g}\left(\frac{\omega^2_{\vec{k}_1+\vec{k}_2}}{g} + \frac{\omega^2_{\vec{k}_1+\vec{k}_3}}{g} + \right.\right.$$
$$\left.\left.\frac{\omega^2_{\vec{k}-\vec{k}_2}}{g}\frac{\omega^2_{\vec{k}-\vec{k}_3}}{g}\right)\right)\overline{\psi}\overline{\eta}_2\overline{\eta}_3\delta\left(\vec{k}_1 + \vec{k}_2 + \vec{k}_3 - \vec{k}\right) d\vec{k}_1 d\vec{k}_2 d\vec{k}_3 + \ldots = 0$$

$$\overline{\psi} + g\overline{\eta} - \frac{1}{4\pi}\iint\left(\frac{\omega_1^2}{g}\frac{\omega_2^2}{g} + \vec{k}_1.\vec{k}_2\right)\overline{\psi}_1\overline{\psi}_2\delta\left(\vec{k}_1 + \vec{k}_2 - \vec{k}\right) d\vec{k} d\vec{k} - \quad (21)$$
$$\frac{1}{16\pi^2}\iiint\left(2k_1^2\frac{\omega_2^2}{g} + 2k_2^2\frac{\omega_1^2}{g} - \frac{\omega_1^2}{g}\frac{\omega_2^2}{g}\left(\frac{\omega^2_{\vec{k}_1+\vec{k}_3}}{g} + \frac{\omega^2_{\vec{k}_2+\vec{k}_3}}{g} + \right.\right.$$
$$\left.\left.\frac{\omega^2_{\vec{k}-\vec{k}_2}}{g} + \frac{\omega^2_{\vec{k}-\vec{k}_1}}{g}\right)\right)\overline{\psi}_1\overline{\psi}_2\overline{\eta}_3\delta\left(\vec{k}_1 + \vec{k}_2 + \vec{k}_3 - \vec{k}\right) d\vec{k}_1 d\vec{k}_2 d\vec{k}_3 - \ldots = 0$$

Equation 20 and 21 are combined into a single equation by introducing the complex function b given by (22):

$$b\left(\vec{k},t\right) = \sqrt{\frac{g}{2\omega}}\overline{\eta}\left(\vec{k},t\right) + i\sqrt{\frac{\omega}{2g}}\overline{\psi}\left(\vec{k},t\right) \quad (22)$$

From that moment, we define the Fourier transforms of η and $\psi(x,y,t)$ as function of b and its conjugate b*.

$$\overline{\eta}\left(\vec{k},t\right) = \sqrt{\frac{\omega}{2g}}\left(b\left(\vec{k},t\right)\right) + b^*\left(-\vec{k},t\right) \quad (23)$$

$$\overline{\psi}\left(\vec{k},t\right) = i\sqrt{\frac{g}{2\omega}}\left(b\left(\vec{k},t\right) + b^*\left(\vec{k},t\right)\right) \quad (24)$$

Then multiplied (Equation 20) by $(g/2\omega)^{1/2}$ and (Equation 21) by $(i(\square/2g)^{1/2})$. Sums of the terms are given by (25).

$$b_t + i\omega b + i\iint V^1\left(\vec{k},\vec{k}_1,\vec{k}_2\right)b_1 b_2 \delta\left(\vec{k} - \vec{k}_1 - \vec{k}_2\right) d\vec{k}_1 d\vec{k}_2 + \quad (25)$$
$$i\iint V^2\left(\vec{k},\vec{k}_1,\vec{k}_2\right)b_1^* b_2^* \delta\left(\vec{k} + \vec{k}_1 - \vec{k}_2\right) d\vec{k}_1 d\vec{k}_2 +$$
$$i\iint V^3\left(\vec{k},\vec{k}_1,\vec{k}_2\right)b_1^* b_2^* \delta\left(\vec{k} + \vec{k}_1 + \vec{k}_2\right) d\vec{k}_1 d\vec{k}_2 +$$
$$i\iiint W^1\left(\vec{k},\vec{k}_1,\vec{k}_2,\vec{k}_3\right)b_1 b_2 b_3 \delta\left(\vec{k} - \vec{k}_1 - \vec{k}_2 - \vec{k}_3\right) d\vec{k}_1 d\vec{k}_2 d\vec{k}_3 +$$
$$i\iiint W^2\left(\vec{k},\vec{k}_1,\vec{k}_2,\vec{k}_3\right)b_1^* b_2 b_3 \delta\left(\vec{k} + \vec{k}_1 - \vec{k}_2 - \vec{k}_3\right) d\vec{k}_1 d\vec{k}_2 d\vec{k}_3 +$$
$$i\iiint W^3\left(\vec{k},\vec{k}_1,\vec{k}_2,\vec{k}_3\right)b_1^* b_2^* b_3 \delta\left(\vec{k} + \vec{k}_1 + \vec{k}_2 - \vec{k}_3\right) d\vec{k}_1 d\vec{k}_2 d\vec{k}_3 +$$
$$i\iiint W^4\left(\vec{k},\vec{k}_1,\vec{k}_2,\vec{k}_3\right)b_1^* b_2^* b_3^* \delta\left(\vec{k} + \vec{k}_1 + \vec{k}_2 + \vec{k}_3\right) d\vec{k}_1 d\vec{k}_2 d\vec{k}_3 + \ldots = 0$$

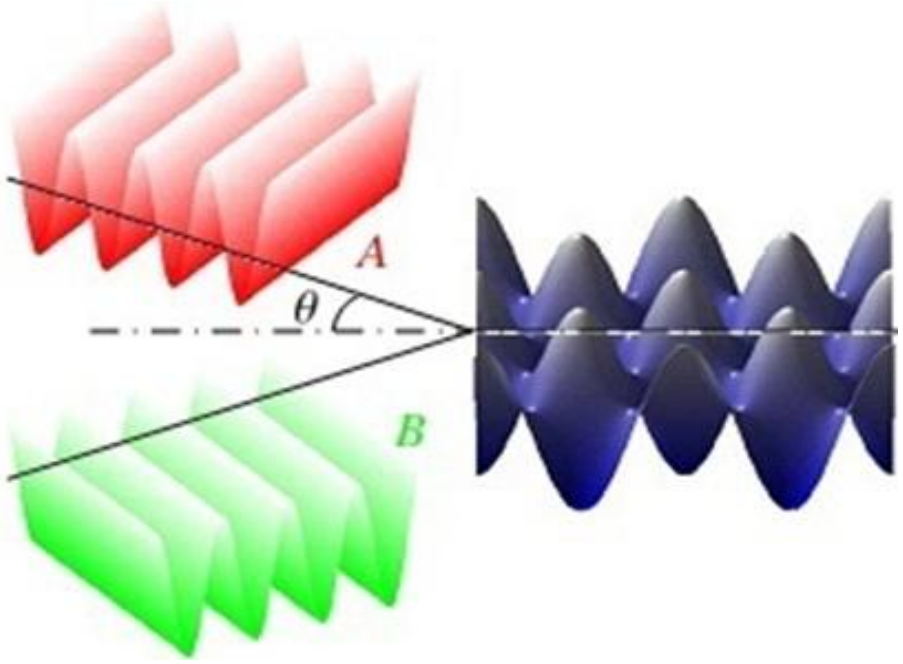

Figure 2. Colliding of two surface waves at an angle θ.

In Equation 26 below, the surface wave $b(\vec{k},t)$ is decomposed into a principal component B and two minor components B' and B'': these components are all functions of t, $t_1= \varepsilon t$ and $t_2=\varepsilon^2 t$.

$$b\left(\vec{k},t\right)=\left(\varepsilon B\left(\vec{k};t,t_1,t_2\right)+\varepsilon^2 B'\left(\vec{k},t,t_1,t_2\right)+\varepsilon^3 B''\left(\vec{k},t,t_1,t_2\right)\right)e^{(-i\omega_k t)} \quad (26)$$

We derive the surface wave (26) with respect to time and substituted in (25). Then taking $\beta = \varepsilon.B$, we obtain what we call the Zakharov integral equation (Equation 27).

$$i\beta_t=\iiint T_{0,1,2,3}\beta_1^*\beta_2\beta_3\delta\left(\vec{k}+\vec{k}_1-\vec{k}_2-\vec{k}_3\right)e^{i(\omega_0+\omega_1-\omega_2-\omega_3)t}d\vec{k}_1 d\vec{k}_2 d\vec{k}_3 \quad (27)$$

METHODOLOGY AND APPROACH

Determination of the coupled nonlinear Schrödinger equations (CNLSE)

According to the nonlinear Schrödinger equation (NLSE), the evolution of an unstable wave group generates a single wave that can reach up to 3 times the amplitude of the initial carrier wave (that is, the wave energy is basically concentrated in a single wave number). Let us consider a surface wave whose main component □ is of the form $\beta = a(k,t).e^{-i\omega.t}$, then Zakharov's integral equation for this type of wave has the form:

$$\frac{\partial a_1}{\partial t}+i\omega a_1=-i\int T_{1,2,3,4}\delta\left(\vec{k}_1+\vec{k}_2-\vec{k}_3-\vec{k}_4\right)d\vec{k}_1 d\vec{k}_2 d\vec{k}_3 \quad (28)$$

We consider the case of energy concentrated mainly around two-wave numbers (Figure 2):

$$a\left(\vec{k}\right)=A\left(\vec{k}-\vec{k}_{(a)}\right)e^{-i\omega_{(a)}t}+B\left(\vec{k}-\vec{k}_{(b)}\right)e^{-i\omega_{(b)}t} \quad (29)$$

Where A and B satisfy the CNLSE (Grönlund et al., 2009; Zakharov et al., 2006):

$$\frac{\partial A}{\partial t}=-C_x\frac{\partial A}{\partial x}-C_y\frac{\partial A}{\partial y}+i\left(\tau\frac{\partial^2 A}{\partial x^2}+\varsigma\frac{\partial^2 A}{\partial y^2}+\vartheta\frac{\partial^2 A}{\partial x\partial y}\right)-i\left(\xi|A|^2A+2\zeta|B|^2A\right) \quad (30)$$

$$\frac{\partial B}{\partial t}=-C_x\frac{\partial B}{\partial x}-C_y\frac{\partial B}{\partial y}+i\left(\tau\frac{\partial^2 B}{\partial x^2}+\varsigma\frac{\partial^2 B}{\partial y^2}+\vartheta\frac{\partial^2 B}{\partial x\partial y}\right)-i\left(\xi|B|^2B+2\zeta|A|^2B\right) \quad (31)$$

We now consider the following plane wave solution of CNLSE:

$$A= A_0.(1+a).e^{-i(\omega.t+\Phi a)}\ ,\ B= B_0.(1+b).e^{-i(\omega.t+\Phi b)} \quad (32)$$

Where a, b, Φ_a, Φ_b are small perturbations in amplitude and of the wave solution. We substitute (32) in (30) and (29), then linearize the resulting equations and use the normal mode approach, with the

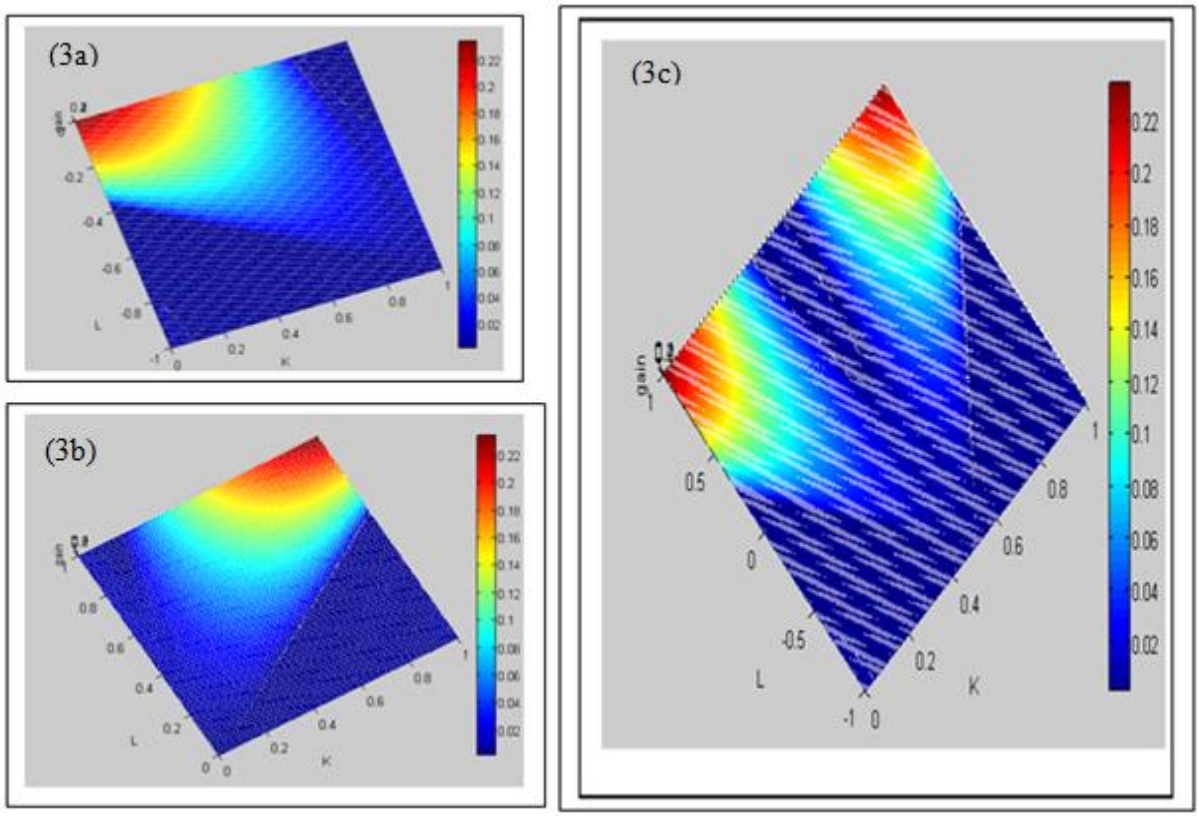

Figure 3. The normalized growth rate « Gain » plotted as a function of (K,L). Here we have used $\theta = \pi/8$, then rotate the figure to get an idea of the evolution of L and K for a fixed value of "Gain". The left-hand panels show the cases with single waves while the right-hand panel shows the case of interacting waves.

wave number, $\vec{K}(K,L)$ and the angular frequency (Ω) of the perturbation, to obtain the following dispersion equation:

$$\Omega = \pm\sqrt{\pi K^2\left[(\xi\left(A_0^2 + B_0^2\right) + \pi K^2) \pm \sqrt{\xi^2\left(A_0^2 - B_0^2\right)^2 + 16\zeta^2 A_0^2 B_0^2}\right]} \quad (33)$$

Approach

Calculations are performed by a MATLAB program. The curves are shown in 3D and can be rotated according to our desire. The choice of the number of iteration involved 200 instead of 100 (which produced figures with color coding irrelevant).

RESULTS AND DISCUSSION

In the following, we numerically solve our nonlinear dispersion relation (33) and investigate the full dynamics of nonlinearly interacting deep water waves subjected to modulation or filamentation instabilities. After that, we present the growth rate "gain" (the imaginary part of Ω in Figures 3, 4, 5 and 6, where we have studied the impact of different angles θ on the growth rates for interacting waves. In the left-hand panels of Figure 3a, b and c and Figure 4 a, b and c, we show the single wave cases, which exhibit the standard Benjamin-Feir instability (Segur et al., 2005) tilted by the angle θ in the (K,L) plane. The right-hand panels show the cases of interacting waves. We can see from Figure 3c that a relatively small $\theta = \pi/8$ gives rise to a new instability with a maximum growth rate of more than twice as large as that of the single cases, in the direction of the dichotome. For a larger angle $\theta = \pi/4$, displayed in Figure 4c, we see that the two waves do not interact to enhance the linear growth rate significantly.

One can also observed that, in Figure 6c (where $\theta = \pi/3$), the two waves do not interact to enhance the growth rate significantly. While in figure 5c, where the angle θ is equal to $\pi/6$, the waves interact much more, the gap between the two superposed surface waves, characterized by dark blue, is more pronounced in Figure 6c than in Figure 5c.

Obviously the rogue waves are generated by primary waves whose directions of propagation are nearly parallel (that is, $0 < \theta < \pi/6$). This ensures their unexpected character (expressed by the quasi-spontaneous passage from a calm situation to a sea greatly agitated). All these

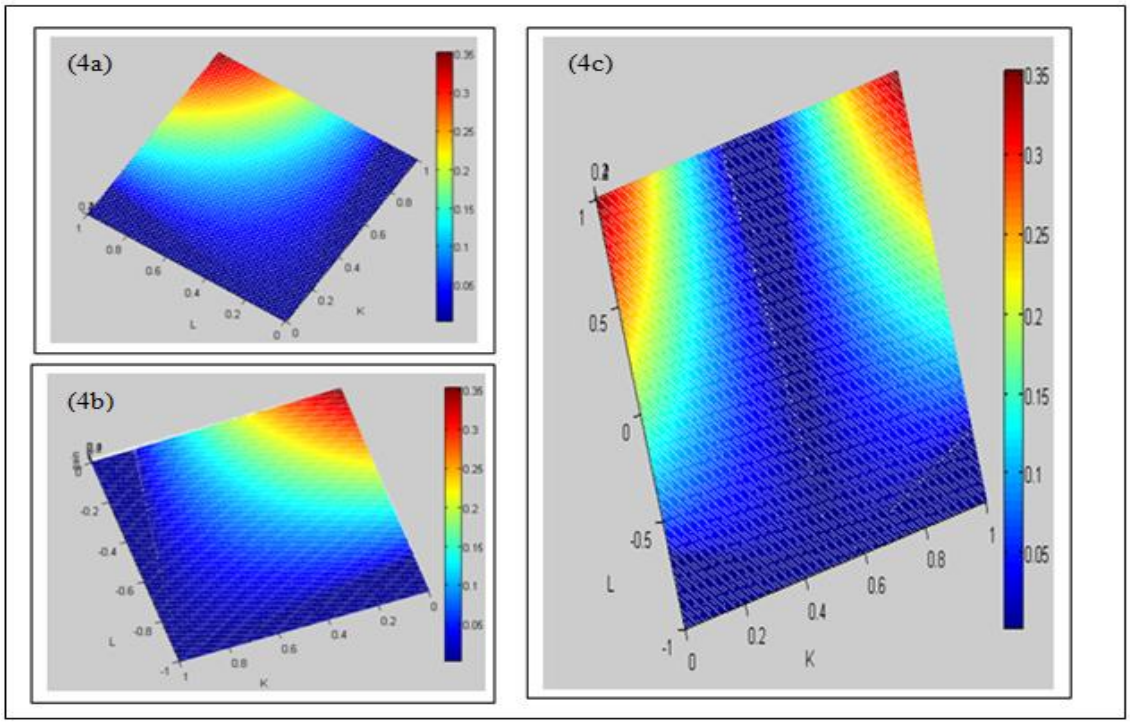

Figure 4. The normalized growth rate « Gain » plotted as a function of (K,L). Here we have used $\theta = \pi/4$, then rotate the figure to get an idea of the evolution of L and K for a fixed value of "Gain". The left-hand panels show the cases with single waves while the right-hand panel shows the case of interacting waves.

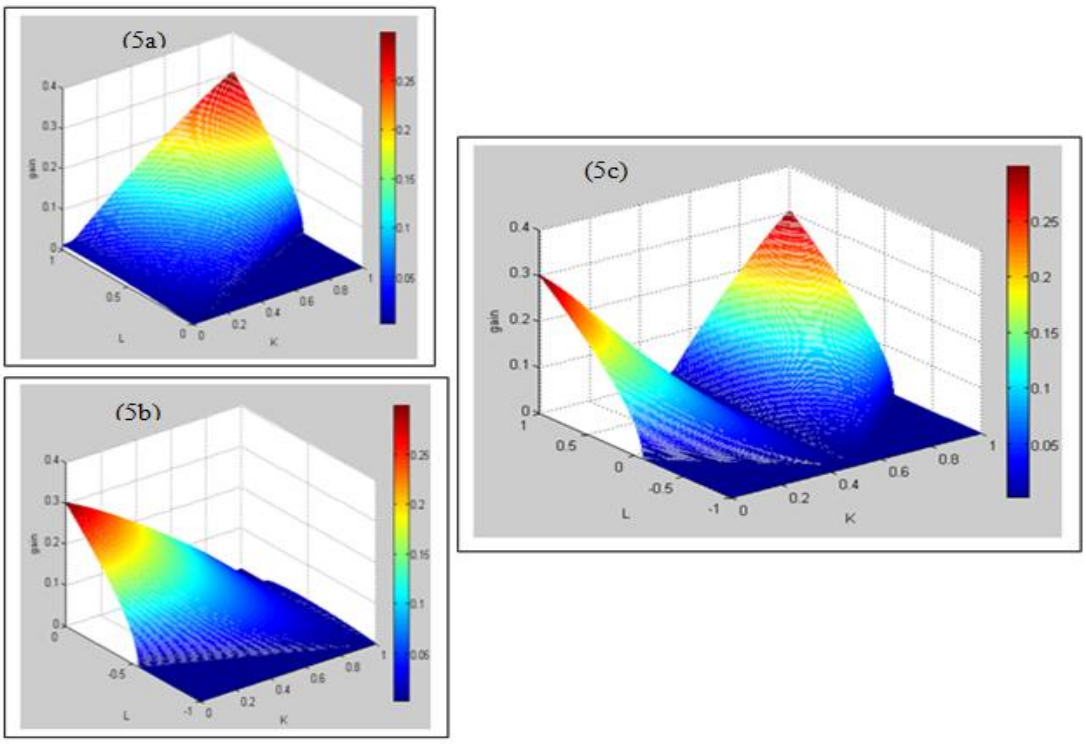

Figure 5. The normalized growth rate « Gain » plotted as a function of (K,L). Here we have used $\theta = \pi/6$. The left-hand panels show the cases with single waves while the right-hand panel shows the case of interacting waves.

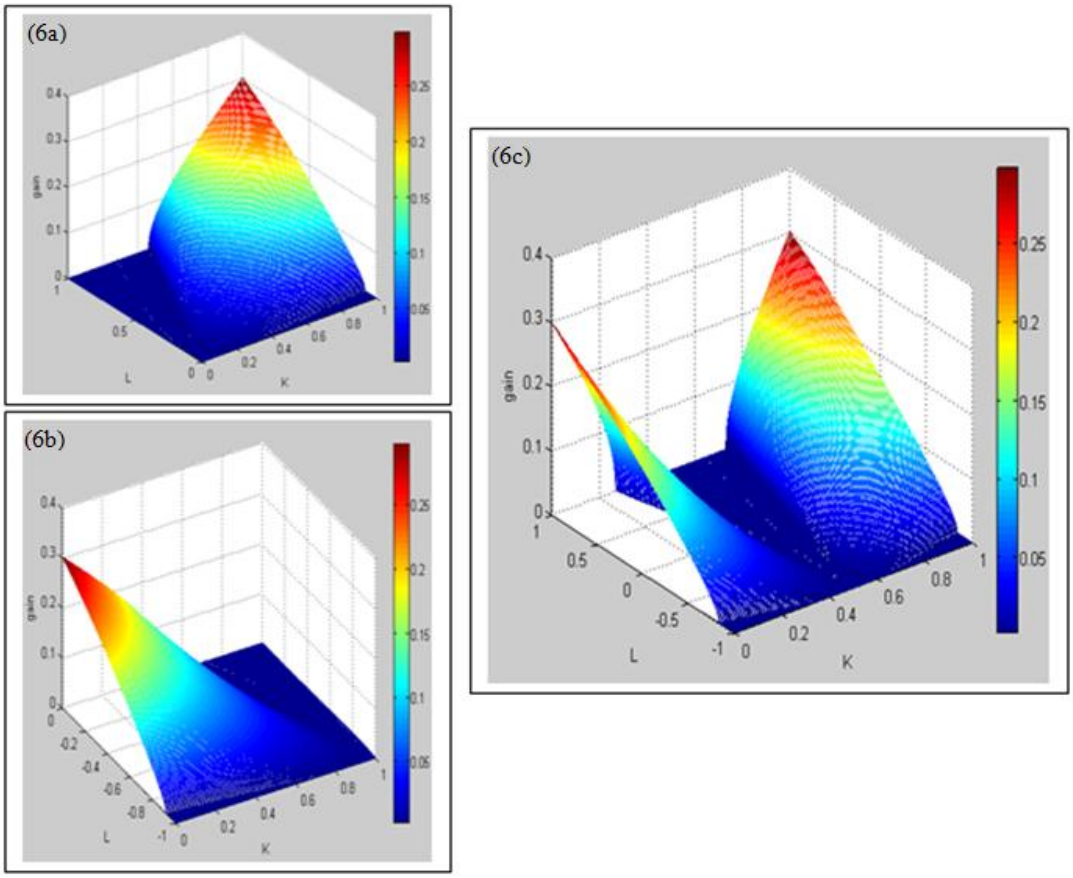

Figure 6. The normalized growth rate « Gain » plotted as a function of (K,L). Here we have used $\theta = \pi/3$. The left-hand panels show the cases with single waves while the right-hand panel shows the case of interacting waves.

results will have relevance to the nonlinear instability of colliding water waves, which may interact nonlinearly in a constructive way to produce large amplitude freak waves in the oceans.

Conclusion

The existence of rogue waves is universally recognized and images on the extent of the damage caused by these monsters of the ocean are available online on the Internet. However, the physical processes responsible for the formation of these phenomena as well as its prediction are not completely understood. This paper shows that rogue waves are a combination of complex processes that occur under accuracy conditions like interference between primary waves whose directions of propagation are nearly parallel. Rogue waves are not waves that appear from nowhere and disappear without trace as stated by some authors: according to the NLSE, the evolution of an unstable wave group generates a single wave that can reach up to 3 times the amplitude of the initial carrier wave (that is, the wave energy is basically concentrated in a single wave number). Our paper presents the application of Zakharov equation in three dimensions (to deep water gravity waves, which is an important tool for acquiring information on the scientifically conceivable reasons for the formation of rogue waves. In this regard, additional assumptions are implemented to make the transition from hydrodynamic Euler equations to Zakharov's modulation instability. Considering only deep rivers (H tends to infinity), we try to avoid interactions between the bottom and the surface of the rivers (where the waves are located): stories describing the rogue waves, do not mention the appearance of ocean volcanoes. The same precautions recommended considering only very large rivers. This prevents interference between the primary waves and those produced by their reflection on the shores. The results presented are new, clear and neat. But they only consider the energy point of view: this means that only amplitude modulations are processed. We are currently working on phase modulations, to try to understand more about rogue waves.

Symbols

Physical symbols

b : Complex surface function
B_i: Main component of the complex surface function (i = 0,1,2,3)
B_i: Smaller component of the complex surface function (i = 0,1,2,3)
B_i: Smallest component of the complex surface function (i = 0,1,2,3)
g: Acceleration due to gravity
$\vec{g}$: Three – dimensional acceleration due to gravity
H: Water depth
k_i: Wave number (i = 0,1,2,3)
$\vec{k}_i$: Wave number vector (i = 0,1,2,3)
P: Pressure
t: fast time scale
t_1: Slower time scale
t_2: Slowest time scale
V_i: Interaction coefficient (i = 0,1,2,3)
w: Vertical velocity of particle
W_i: Interaction coefficient
$\beta(ki) = \beta_i$: Main component of the complex surface function (i = 0,1,2,3)
ε: Measure of non-linearities (steepness)
ϕ: Velocity potential
η: Surface elevation
η_t: Derivative of the surface elevation η with respect to time
ψ: Stream function
ψ_t: Derivative of the stream function ψ with respect to time
$\omega(k_i) = \omega_i$: Angular frequencies of interaction waves

Mathematical symbols

δ: Dirac's δ – function
$\vec{\nabla}$: Three – dimensional gradient
$\vec{\nabla}_\perp$: Vertical component of the gradient
*: complex conjugate

Dispersion coefficients

$C_{x,\,y}$= Group velocity components
$\tau,\varsigma,\vartheta,$= Group dispersion coefficients
ξ= Non-linear coefficient
ζ= Coupling coefficient

REFERENCES

Atock ANS, Mbane C, Ekobena FH (2010). Lattice Bolzmann simulation of the two – dimensional poiseuille – Rayleigh – Benard flows instability. IJPS., 5(7): 984-991.

Batra K, Sharma RP, Verga AD (2006). Stability analysis on nonlinear evolution paterns of modulational Zakharov equations. J. Plasma Physis., 72: 671-686.

Chambarell J (2009). Etude des vagues extrêmes en eau peu profonde. Thèse de Doctorat de l'Université de Provence Aix-Marseille.

Dyachenko AI, Zakharov VE (2005). Modulational instability of Stokes wave – freak wave. J. Exp. Theor. Phys., 81(6): 318-322.

Kharif C, Pelinovsky E (2003). Physical mechanism of the rogue wave phenomenon. European J. Mechanics/B-Fluid. 22(6): 603-634.

Leblanc S (2008). Wind – forced modulations of finite – deph gravity waves, Phys. Fluid, 20: 116603.

Mbane BC (2009). Vertical profiles of winds and electric fields triggered by tropical storms – under the hydrodynamic concept of air particle. IJPS., 4(4): 242-246.

Onorato M, Osborne AR, Serio M, Cavaleri L, Stanberg TC (2004). Observation of strongly non-Gaussian statistics for random sea surface gravity waves in wave flume. Phys. Rev., E 70: 067302.

Socquet H, Juglar A, Dysthge K, Trulsen K, Krogstad HE, Liu J (2005). Probability distributions of surface gravity waves during spectral change. J. Fluid Mech., 542: 195.

Shener L (2010). On Benjamin – Feir instability and evolution of non – linear wave with finite – amplitude side bands, Nat. Hazards Earth Syst. Sci., 10: 2421-2427.

Touboul J (2007). Etude de l'Interaction entre le vent et les vagues scélérates. Thèse de Doctorat de l'Université de Provence Aix-Marseille.

White BS, Fornberg B (1998). On the chance of freak waves at sea. J. Fluid Mech., 355: 113-138.

Wu CH, Yao A (2004). Laboratory measurements of limiting freak waves on current. J. Geophys.Res., 109(C 12002): 1 -18.

Yuen, Lake (1980). Instability of Waves on Deep Water. Ann. Rev. Fluid Mech., 12: 303-334.

Zakharov VE (1968). Stability of Periodic waves of finite amplitude on the surface of a deep fluid, Zhumal Prikladnoi Mekhaniki 1Tekhnicheskoi, 9(2): 86-94.

Zakharov VE, Kharitonov (1970). Instability of Periodic Waves of Finite Amplitude on the Surface of a Deep Fluid. Zh. Prikl. Mekh.1Tekhn.Fiz, 9: 45-49.

Zakharov VE, Dyachenko A, Prokofiev AO (2006). Eur. J. Mech. B/ Fluids, 25: 677.